Materials Research. 2024; 27:e20230538
DOI: https://doi.org/10.1590/1980-5373-MR-2023-0538

Microstructural and Mechanical Property Analyses of Ti/Al/Ti Laminated Composites Prepared by Ultrasonic Welding

Yifu Zhang[a]*, *Zhanzhan Su*[a,b], *Deqin Zhang*[a], *Zhengqiang Zhu*[b]

[a]*Jiujiang University, School of Materials Science and Engineering, Jiangxi Province Engineering Research Center of Materials Surface Enhancing & Remanufacturing, Jiujiang 332005, China.*
[b]*Nanchang University, School of Advanced Manufacturing, Key Laboratory for Robot & Welding Automation of Jiangxi Province, Nanchang 330031, China.*

Received: December 08, 2023; Revised: May 19, 2024; Accepted: July 01, 2024

Ti/Al/Ti laminated composite material is an ideal material for high-temperature parts and protective armor in the aerospace field because of its high specific strength and high temperature oxidation resistance. To improve the joint strength, the ultrasonic welding solid-phase joining technology is used to prepare Ti/Al/Ti laminated composites. The results show that the temperature, microstructure and microhardness distribution of the aluminum interlayer are uniform after welding. The recovery recrystallization behavior reduces the hardness of the aluminum interlayer during welding, while the microstructure and microhardness of the upper and lower titanium layers do not change significantly. The tensile shear failure positions of the joints are all located in the lower Al/Ti interface layer, and the highest tensile shear strength reaches 124.4 MPa (1200 W). At this parameter, the plastic constraint reinforcement effect is the most significant, the interface exhibits a small amount of vortex-like morphology, and the local area of the aluminum material melts below the equilibrium melting point. When the welding power reaches 1400 W, the upper surface of the weld is crushed, and the $TiAl_2$ IMC phase precipitates in the Ti/Al interface region.

Keywords: *Ti/Al/Ti laminated material, ultrasonic welding, microstructure, constraint reinforcement effect, IMC phase.*

1. Introduction

Connecting structural components with dissimilar materials can reduce manufacturing costs while harnessing the performance advantages of different materials, thereby achieving a performance-balanced structure that meets various working conditions. For example, aluminum alloys are characterized by their low cost and density, while titanium alloys are characterized by their high strength and corrosion resistance. A combination of these two materials is widely used in industrial fields, such as aerospace and automotive applications[1]. However, there are significant differences in the performance of titanium alloys and aluminum alloys, which are reflected in physical properties, such as melting point, thermal conductivity, coefficient of linear expansion, and crystalline chemical properties, making it challenging to obtain high-quality welding joints. Especially during the fusion welding process, hard and brittle intermetallic compounds (IMCs) formed in the Ti-Al system tend to precipitate at the welding interface[2,3]. Therefore, the low-temperature effects of solid-state joining techniques are suitable for connecting dissimilar metal materials, such as diffusion welding, explosion welding, and various types of friction welding techniques[4,5]. The solid-state welding techniques are characterized by low peak temperature, severe plastic deformation, energy efficiency and nonpollution, which can simultaneously realize the mechanical and chemical bonding, improving mechanical performances[6]. However, when welding Ti/Al dissimilar materials, it is difficult to avoid the precipitation of IMCs, and effective joint connections can be achieved when the critical thickness does not exceed 5 μm[7].

Ultrasonic spot welding (USW) is a solid-state forming technique that enables the connection of both similar and dissimilar low-melting-point nonferrous metal thin sheets. Compared with other solid-state forming techniques, USW has specific advantages, such as low energy consumption (several times lower than friction welding and resistance welding), short welding times, and low requirements for the welding surface. The strength of the welded joints achieved through ultrasonic welding is comparable to the strength obtained by other welding methods. During the ultrasonic welding process, the peak temperature in the interface region is much lower than the melting point of the base material, and it is believed that the temperature range for reliable connections lies between 25% and 75% of the melting point temperature of the base metal[8]. The experimental results by Zhou et al.[9] indicate that during the ultrasonic welding process of CP Ti/AA6061 aluminum alloy, the highest interface temperature reaches 365 °C. Zhang et al.[10,11] conducted high-power ultrasonic welding experiments on AA6111, AA2139 aluminum alloys, and Ti_6Al_4V titanium alloy separately, and the results show that the highest interface temperature is below 540 °C. Balle and

*e-mail: zhangyifu_lab@126.com

Magin[12] conducted experimental research on the formation of mixed interfaces in Ti/Al ultrasonic welding and identified the possible presence of four different types of interfaces: Al-Al_2O_3 and/or TiO_2-Ti. However, none of the above experiments have shown precipitation of the IMC phase at the Ti/Al weld seam, which is attributed to the low welding energy, transient action time, and high diffusion activation energy associated with Ti/Al ultrasonic welding. Wang et al.[13] studied the influence of an Al interlayer on the performance of ultrasonic-welded joints between Al5754-O aluminum alloy and Ti_6Al_4V titanium alloy. The scholars found the presence of the $TiAl_3$ IMC phase in a very narrow region of the weld seam after adding the Al interlayer, suggesting that the peak interface temperature during the welding process exceeds the melting point of Al. However, the researchers did not experimentally measure the interface temperature. In cases where the ultrasonic welding frequency and time are the same, it has been observed that the strength of Ti/Al dissimilar metal weld joints is similar when welding at a pressure of 0.55 MPa with a welding energy of 2000 J relative to welding at a pressure of 15 MPa with a welding energy of 4000 J[9,10]. This finding indicates that solely adjusting the ultrasonic welding process parameters cannot further enhance the mechanical performance of Ti/Al joints. This phenomenon is primarily due to significant differences in the physical and chemical properties of dissimilar metals, poor metallurgical compatibility, narrow welding process window, and low robustness. Furthermore, the high melting point and hardness characteristics of titanium alloys make it challenging to achieve effective connections through ultrasonic welding. Achieving a connection may come at the cost of significantly weakening the load-bearing surface of the joint.

With the advancement of aerospace technology, single-layer high-strength titanium alloys are gradually being replaced by layered composite materials with superior performance. Relative to single materials, these layered composite materials can effectively enhance toughness, and the gradient combination formed can reduce the impact load, thereby improving the secondary load-carrying capacity. Ti/Al/Ti layered composite materials, due to their high specific strength and good high-temperature oxidation resistance, are ideal composite materials for high-temperature components and protective armor in the aerospace industry[14,15]. In this regard, the use of ultrasonic welding technology to prepare such layered composite materials is proposed by adding soft aluminum alloy between titanium alloys. The welded component forms a sandwich structure with a hard layer and a soft layer, which can generate a constraint strengthening effect. This effect occurs when the adjacent strong and hard parts of the soft layer constrain and strengthen each other, resulting in strain strengthening. The dependency relationship between the microstructure and mechanical properties of welded joints was established through analysis of interface temperature, microstructure, and mechanical properties. The influence of ultrasonic welding process parameters on joint performance and interface reaction was obtained. The experimental research on the mechanism of Ti/Al/Ti interface formation and constraint strengthening effect has engineering application value in studying dissimilar metal ultrasonic welding theory and the fundamental properties of layered structural materials.

2. Experimental Materials and Methods

The experimental materials used are annealed TA1 Ti (impurity contents: 0.33 Al, 0.1 Fe, 0.05 C, 0.01 H, 0.1 O, 0.03 N, and 0.1 Si (wt.%)) and 1060 Al (impurity contents: 0.35 Fe, 0.25 Si, 0.05 Zn, 0.05 Cu, 0.05 V, 0.03 Mg, 0.03 Ti, and 0.03 Mn (wt.%)). Both materials have dimensions of 100 mm × 20 mm × 0.2 mm. TA1 Ti is composed of equiaxed α-phase grains with a grain size of approximately 8 μm, a tensile strength of approximately 352.7 MPa, and a micro-Vickers hardness of 220 $HV_{0.025\ kg}$. 1060 Al consists of α-triple-phase and acicular hard brittle phases, with a grain size of approximately 50 μm, a tensile strength of approximately 110 MPa, and a micro-Vickers hardness of 30 $HV_{0.025\ kg}$. These two materials exhibit significant differences in mechanical properties. During welding, the base materials are alternately placed, leading to a typical constraint strengthening effect. Although the surface effect of ultrasonic welding can clean the bonding interface, the accumulation of oxides at the interface can be a source of defects, such as cracks and voids. These defects can decrease the bonding efficiency and mechanical performance levels of layered composite materials. Therefore, pretreatment of the base material surfaces is necessary. The prewelding pretreatment involves the use of a 5~10 wt% NaOH aqueous solution to remove surface oxides from the welding base materials. Then, the surface is polished with #320 SiC sandpaper until it exhibits a metallic luster, which is followed by degreasing with acetone.

The experiment is conducted using an NC-2020A ultrasonic welding machine with the following parameters:

1. 1060 Al is placed between TA1 Ti to prevent the aluminum alloy from sticking to the sonotrode and anvil surfaces and to create a hard–soft sandwich structure.
2. The welding force (F) is 1150 N, providing a static pressure of approximately 12.8 MPa, which is approximately 85% of the room temperature yield strength of 1060 Al.
3. The welding power (P) is 800 W~1400 W, which is increased in increments of 200 W.
4. The welding time (t) is 600 ms.
5. The weld joint area (S) is 15 × 6 mm^2.
6. The ultrasonic vibration frequency (f) is 20 kHz.

To ensure proper alignment of the workpiece surfaces with the bottom and top layers, the sonotrode and the anvil surface have side teeth. These teeth efficiently transfer ultrasonic energy and ensure effective friction at the interface. The three stages of interface connection point growth, workpiece joint form, ultrasonic sonotrode morphology and typical welding specimen appearance are shown in Figure 1.

The specimens for observation and testing are first obtained by wire cutting and then subjected to grinding, mechanical polishing, and chemical polishing while being placed on a suspension of SiO_2 with a particle size of 0.03~0.04 μm. The microstructure and composition distributions of cross-sections are analyzed in the vertical vibration plane using backscattered electron (BSE) mode and energy-dispersive

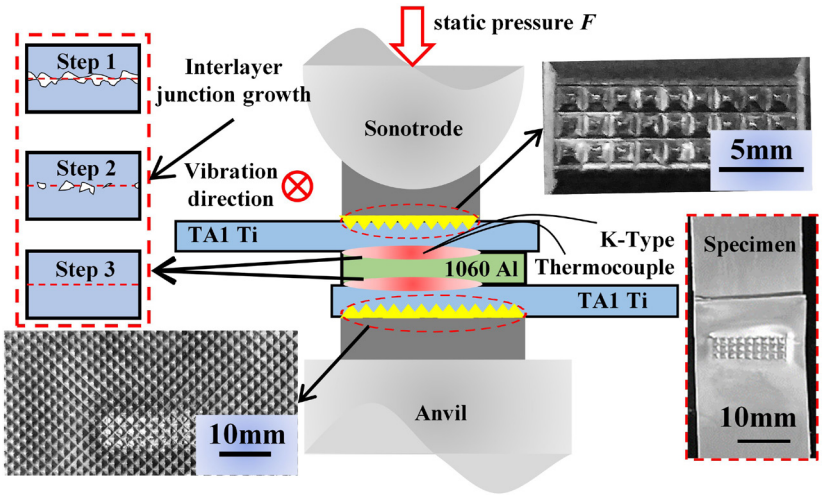

Figure 1. Schematic diagram of the ultrasonic welding process and the appearance of a welded specimen.

X-ray spectroscopy (EDS) on a TESCAN VEGA II scanning electron microscope (SEM). The interface phase composition is analyzed using a Rigaku D/max-2400 X-ray diffractometer (XRD) with a step size of 0.05° and a scanning range of 20° to 90°. The peak temperature at the center of the weld seam is measured using a K-type thermocouple with a scanning speed of 100 ms/channel (equipment model: AT4508). The microhardness of the layered composite material is characterized using a microhardness tester (equipment model: HXD-1000TM/LCD) with a load of 0.025 kg and a dwell time of 10 s. To ensure measurement accuracy, at least 5 average hardness values are taken from points near the weld seam, and the standard deviation is used as the measurement error. The Hysitron TI980 TriboIndenter type high-precision nanomechanical testing system is used to test the nanohardness and load-displacement curve (p-h curve). In-situ scanning probe microscopy is used to scan and obtain the 3D morphology to determine the plastic deformation behavior around the indentation. Load control mode: force loading mode, maximum loading force 8000μN, loading rate 300μN/s. To analyze the shear force under different welding powers (joint shear strength can be estimated by dividing the maximum load by the welding cross-sectional area of 9 mm^2. The estimated reason is that during high-power welding, the joint surface is crushed, leading to errors in the bearing surface.), tests are conducted at room temperature using a universal testing machine in accordance with BS EN ISO 9018:2015 (equipment model: WDW3050; testing parameters: loading speed of 1 mm/min).

3. Results and Discussion

3.1. Weld microstructure

Accurately measuring the trend of temperature variation at the welding interface is crucial for determining microstructural evolution characteristics. To achieve this accuracy, temperature gradient changes near the weld zone are measured repeatedly. Figure 2 illustrates the thermal distribution at the central region of the upper and lower interfaces of Ti/Al/Ti at different

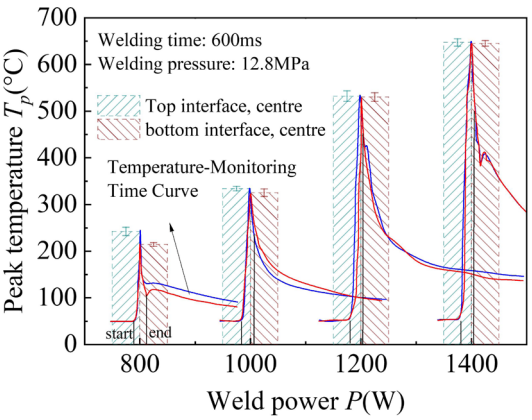

Figure 2. Interfacial heat distribution in the central area of the Ti/Al/Ti top and bottom interfaces at different ultrasonic welding power levels.

power levels. The peak interface temperature increases from approximately 214 °C to approximately 647 °C as the welding power varies from 800 W to 1400 W, which is significantly lower than the melting point temperature of the titanium alloy substrate. Scholars have indicated that it is difficult to form recrystallized grains in the aluminum alloy when the temperature does not exceed 326.85 °C within a very short time frame (2 s)[16]. Intense plastic deformation can lead to the accumulation of dislocations at the welding interface, resulting in a significant increase in the atomic vacancy concentration and diffusion rate in the high-strain plastic deformation around the Ti/Al/Ti upper and lower interface areas during ultrasonic welding. This finding indicates that even in the low-temperature transient welding process of ultrasonic welding, the presence of excess vacancies affects thermodynamic stability, and as a result, recovery recrystallization may occur around the weld seam or localized melting may occur in aluminum alloy regions below their equilibrium melting point. At medium-to-low welding line energies, the microstructure at the Ti/Al interface is primarily influenced by dynamic recovery recrystallization. However,

at relatively high line energies, the microstructure at the Ti/Al interface is mainly affected by interface precipitates. The mechanism of interface formation is primarily based on solid-state bonding driven by atomic interdiffusion. The elevated temperature during welding reduces the strength of the base materials, further facilitating the formation of a bonding interface. The high heating and cooling rate gradients during welding promote grain refinement at the interface and lead to increased thermal stresses. It is observed that with increasing welding power, the temperature difference between the upper and lower interfaces decreases, and the variation in the interface temperature gradually decreases. This phenomenon is related to the progressive thinning of the aluminum alloy layer. Additionally, as the welding heat input increases, the degree of interface bonding increases, leading to the consumption of welding energy due to interface adhesive friction and plastic deformation. This effect occurs because the thermal conductivity of titanium is 13 times that of aluminum and 4 times that of steel (used for the sonotrode and anvil). This characteristic indicates that titanium acts as a thermal insulator, resulting in a relatively uniform temperature distribution within the intermediate layer.

The macrostructure diagrams of the joint cross-sections under different ultrasonic welding powers are shown in Figure 3. According to Figures 3a and 3b, there are no cracks, discontinuities, or porosities in the weld seams. The titanium plate undergoes a wavy plastic deformation, and there is no significant change in thickness dimensions. The deformation zone primarily occurs in the area where the weld tip penetrates the anvil. The aluminum interlayer experiences varying degrees of thinning throughout the weld seam, with the highest reductions in thickness dimensions reaching 38% and 10% of the original dimensions, respectively. The interface between the materials is smooth, and there is no apparent mechanical interlocking. This phenomenon suggests that the welding temperature is overly low, leading to the insufficient softening of the titanium plate and limited plastic flow. It should be noted that the microstructure of the titanium alloy does not undergo significant changes at an annealing temperature of 500 °C. This finding indicates that in the power range of 800 W–1000 W for TA1 titanium welding, the microstructure is approximately consistent with that of the base material. Moreover, at this temperature, the aluminum intermediate layer softens sufficiently, leading to increased plastic flow. Research has shown that aluminum alloys exhibit equiaxed and subgrain structures when cold-rolled at a low temperature of 450 °C, and the formation of this grain structure is accompanied by the decomposition of oversaturated solid solutions and the dispersion of fine particles[17]. The shear deformation and deformation-induced heating effects lead to dynamic recovery and recrystallization behavior in this region during the ultrasonic welding process. As a result, fine equiaxed grains form in the vicinity of the intermediate layer interface and promote atomic interdiffusion,

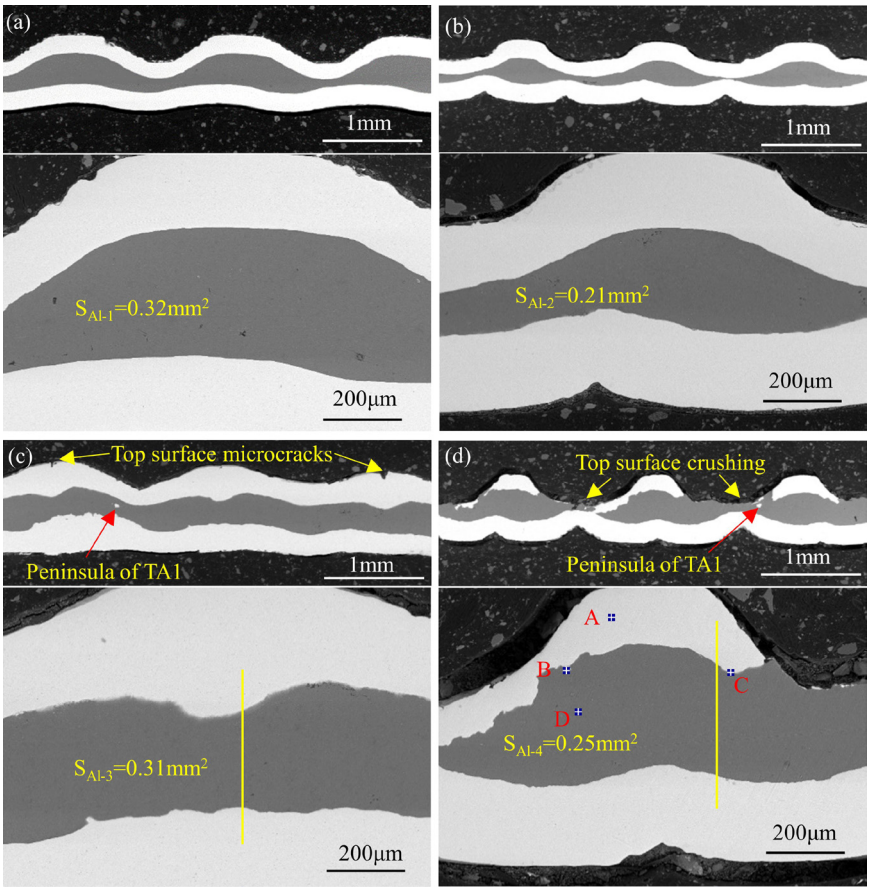

Figure 3. BSE images of the microstructure in the cross-sections of Ti/Al/Ti joints: (a) 800 W, (b) 1000 W, (c) 1200 W and (d) 1400 W.

which facilitates the diffusion of atoms between the materials, leading to the formation of a strong metallurgical bond at the interface.

From Figure 3c, a small number of microcracks appear on the upper titanium surface. These microcracks occur primarily due to the rapid heating and cooling cycle can create thermal stresses in the joint, especially at the top surface peaks, where the heat is concentrated. The low thermal conductivity of titanium alloys increases the possibility of thermal stresses and microcracks formation. In addition, the concentration of high stress formed on both the upper and lower surfaces under alternating shear forces along the vibration direction, while the plastic deformation of the titanium material is insufficient. This combination promotes the formation of cracks on certain surface areas when the load exceeds the fatigue limit. The upper and lower titanium layers exhibit varying degrees of thickening (approaching 207% of the original size). The aluminum intermediate layer shows increased thickness uniformity throughout the weld seam, with the thinnest area being 78% of the original size, and the formation of titanium peninsula areas within the aluminum layer. At the Ti/Al interface, there are some vortex-like morphologies. This morphology indicates that at this temperature, localized melting has occurred in the aluminum material (below its equilibrium melting point). The titanium material softens, and plastic deformation intensifies. Due to the interaction of side teeth on the welding tip and the anvil surface, there is a periodic variation in the form of wave peaks and valleys on the thickness of the welding joint, leading to an uneven characteristic in the thickness of the titanium material. However, due to the even distribution of temperature in the intermediate layer, the high plastic flow of the aluminum layer reduces the magnitude of thickness variations. The high plastic deformation at the interface, along with the formation of subgrains, leads to dislocation accumulation within the base materials. As deformation progresses, recrystallization grains eventually form. This recrystallization behavior further enhances grain refinement on both sides, and the mechanical interlocking effect increases the joint strength. The mechanism of grain refinement in ultrasonic welding mainly includes the following factors: ultrasonic excitation (volume effect) breaks the plate-like grains into smaller-sized grains. Under the influence of interface friction (surface effect), microconvex–concave shear deformation occurs on the aluminum surface, and dislocations accumulate inside the grains, leading to the formation of subgrain boundaries and subsequent recrystallization. This finding illustrates that intense microplastic deformation at the interface and the volume effect of ultrasonic welding significantly impact the evolution of the weld microstructural and mechanical properties. As shown in Figure 3d, with a further increase in welding power, the strength of the titanium plate on the sonotrode side becomes significantly lower than that of the surrounding area due to high-frequency friction and ultrasonic energy (significant high-temperature softening effect). High power input can enhance material plastic flow and create instability at the interface, causing turbulent material flow. On the sonotrode side, this turbulence and the presence of restricted material flow in certain areas can result in uneven distribution of titanium material and potentially push some of the material out of the weld zone. At elevated temperatures, titanium is highly reactive and can form oxides or other compounds rapidly. The oxide layer can spall off by the ultrasonic vibrations, resulting in material loss. This phenomenon leads to the periodic compressive failure of the titanium material on one side (The amount of Ti missing from the top surface crushing zones reaches 67.903%) and the formation of titanium peninsula areas within the intermediate layer, indicating localized melting in the aluminum material.

When considering the overall performance of laminated composite materials prepared through ultrasonic welding, it is necessary to consider factors beyond interfacial atomic diffusion, grain refinement, mechanical interlocking, precipitation phases, and weld defects. The variation in the thickness of the intermediate layer also needs to be considered. This variation occurs because when the layer thickness has not reached its critical proportion, the strength of a laminated composite material primarily depends on the soft intermediate layer. As the proportionate thickness of the intermediate layer decreases, the joint strength increases and gradually approaches that of a titanium plate. This phenomenon is known as the plastic constraint strengthening effect. The mechanism behind this effect is as follows: The aluminum intermediate layer undergoes plastic deformation while being constrained by the upper and lower titanium layers, placing the laminated composite material in a three-way tensile stress state. Under tensile loading, the aluminum layer enters the plastic deformation zone first, while the titanium layers remain in an elastic state. The titanium layers provide a constraining effect on the aluminum intermediate layer, and the level of constraint depends on the variation in thickness proportion.

For this purpose, ImageJ image processing software is used to quantify the postwelding area of the intermediate layer and the ratio of the aluminum layer area to the total area, as shown in Figure 4. The missing data in the statistics arise due to the compressive failure of the upper base material caused by high-power welding. From the graph, the intense plastic flow induced by ultrasonic excitation increases the total joint area in the peak region (In order to measure the area of each layer, the welding length is defined as 2 mm. before welding, S_{total} = 0.6 mm^2). As the welding power increases, the intermediate layer area first decreases and

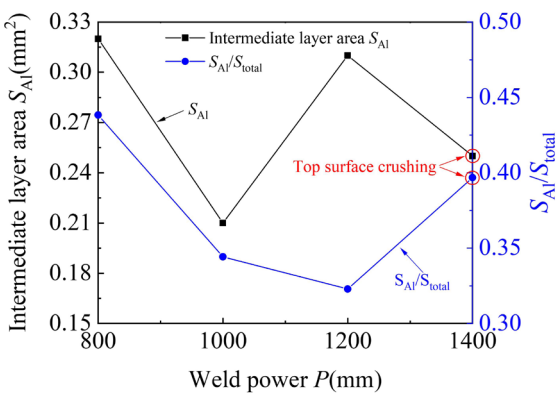

Figure 4. Statistical curve of weld area at different welding powers.

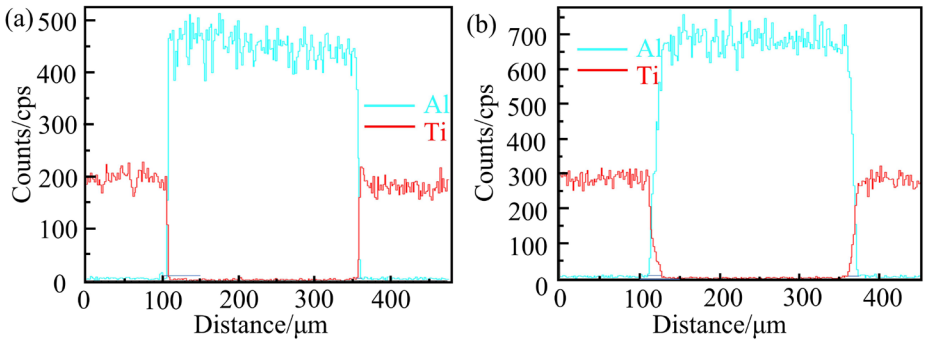

Figure 5. EDS line scan diagram of weld joints: (a) 1200 W and (b) 1400 W.

then increases, with the minimum decreased area being close to the initial area. This trend occurs because at low power levels, there is no significant change in the thickness of the titanium alloy layer. However, as the power increases, the plastic flow in the titanium alloy intensifies, decreasing the ratio of the aluminum layer area to the total area. This finding indicates that the plastic constraint strengthening effect is most significant when the welding power is set to 1200 W.

To analyze the types and distributions of elements at the welding interface, EDS line scanning is performed along the vertical vibration plane (Figure 5), and EDS point scanning is conducted along the high-power weld seam (Table 1). At a welding power of 1200 W, the interface transition zone has a width of approximately 5 μm (the transition sizes of the upper and lower interfaces are similar), which is close to the diameter of the acting component of a scanning electron probe. If the size of the precipitated phase is less than 5 μm, this method may not accurately determine the size of the composition transition zone or whether the IMC phases have precipitated. At a welding power of 1400 W, the upper interface transition zone has a width of approximately 17 μm, and the lower interface transition zone has a width of approximately 13 μm. It can be predicted that when the welding power does not exceed 1200 W, there should be no precipitation of the IMC phases at the interface. However, when the welding power reaches 1400 W, the IMC phases may precipitate at the joint interface. To this end, an analysis is conducted by examining the EDS point scan results at this power level, the Ti-Al binary alloy phase diagram[18], and the Gibbs free energy of possible precipitate phases[19] and by integrating the XRD patterns of interfaces at various power levels to determine the types of phases generated.

During the ultrasonic welding process, Ti and Al atoms at the interface first undergo overheating activation and then deviate from their original lattice positions. Because the atomic radius of Al (0.143 nm) is smaller than that of Ti (0.147 nm), the diffusion rate of Al atoms into TA1 Ti is higher than that of Ti atoms into 1060 Al during the welding process. This finding suggests that Ti atoms can acquire sufficient Al atoms and form bonds with them. To this end, the critical effect for the precipitation phase is the Gibbs free energy of average moles of Ti atoms in IMCs, as shown in Figure 6. A comparison indicates that $TiAl_2$ precipitates first. By combining the EDS results and the binary alloy phase diagram, it can be inferred that at a welding power of 1400

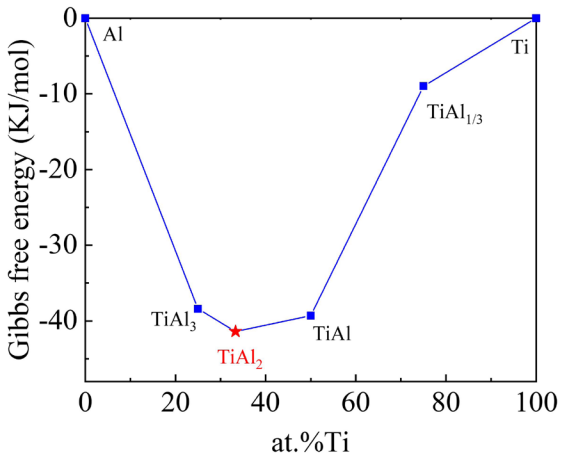

Figure 6. Gibbs free energy curve of the Ti-Al alloy phase.

Table 1. EDS spot scan results of welds at a welding power of 1400 W (at.%).

Position	Ti	Al	Potential precipitate phase
A	99.81	0.19	TA1
B	29.75	70.25	$TiAl_2$+(Al)
C	7.26	92.74	(Al)
D	0.32	99.68	1060 Al

W, the interface (point B in Figure 3d) likely precipitates $TiAl_2$+(Al). Figure 7 shows the interface XRD patterns at different power levels. The figures illustrate that there is no IMC phase precipitation at power levels below 1200 W. However, when the power reaches 1400 W, the $TiAl_2$ diffraction peak can be observed at the interface, which is consistent with the inference.

3.2. Joint mechanical properties

The tensile–shear force–displacement curves of Ti/Al/Ti welded joints at different ultrasonic welding power levels are shown in Figure 8, along with the force–displacement curve of TA1. To compare the strengths of the base material before welding and the Al/Ti ultrasonic welding joint, the unit area failure load after welding, namely, the tensile–shear strength value, is calculated. The estimated tensile–shear strength values corresponding to welding powers of 800 W, 1000 W, 1200 W, and 1400 W are 91.1 MPa, 103.3 MPa, 124.4 MPa,

and 103.3 MPa, respectively. The highest strength is 35.3% of the strength of the Ti base material and 113.1% of the strength of the Al base material. The highest strength is significantly higher than that of the Al/Ti ultrasonic welding joint[9-11]. The results indicate that when the welding power reaches 1200 W, the prepared laminated composite material undergoes recrystallization, grain refinement on both sides of the interface, high atomic interdiffusion in the bonding layer, and no IMC phase precipitation; moreover, there is the presence of mechanical interlocking, and a significant constraint strengthening effect in some area, resulting in high joint tensile–shear strength and good ductility. In this case, except for the excessive power (1400 W), which causes compressive failure of the upper base material and leads to shear failure on the upper side, the joint fails on the lower Al/Ti at all other welding parameters. This result indicates the presence of a strong bond on the upper Al/Ti. This phenomenon occurs due to internal friction and the resulting heat generation causing mechanical energy loss in the upper welding joint, decreasing the efficiency of ultrasonic vibration transmission from the sonotrode to the anvil. After welding, the upper material undergoes warping deformation, increasing the stress concentration in the vicinity of the lower weld seam. In addition, due to the grain refinement, severe plastic deformation and cold-welding effect of the aluminum interlayer after welding, the strength of the interlayer (1060 Al) is improved[20]. The difference in strengths of the upper and lower interfaces can be adjusted by changing the thickness of the upper base material or by changing the shape of the sonotrode to reduce mechanical energy loss and adjust the stress distribution in the joint. Among them, the tensile-shear failure interfacial fracture morphology of the Ti/Al/Ti welded joints at welding powers of 1200 W and 1400 W is shown in Figure 9. At a welding power of 1200 W (Figure 9a), the fracture surface is composed of numerous microscopic dimples and a very small amount of smooth surface, which is a typical ductile fracture mode. At a welding power of 1400 W, the above analysis indicates that the weld contains a small amount of high-hardness $TiAl_2$ phase, which is the weakest part of the joint. It reduces the toughness and crack arrest performance of the joint, leading to a decrease in tensile–shear strength. The corresponding interfacial fracture morphology is shown in Figure 9b. The fracture surface consists of short and curved river patterns, small-area smooth surfaces, radial

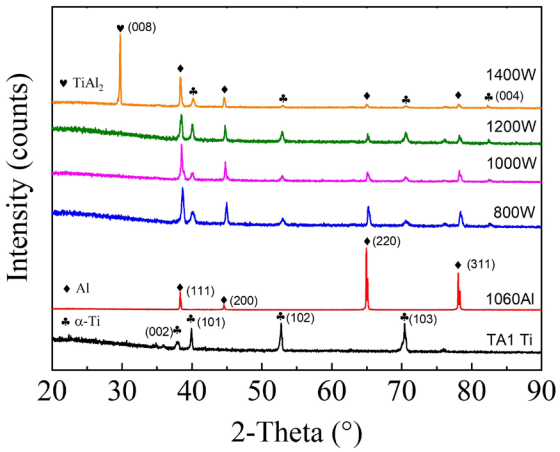

Figure 7. XRD patterns of the interface at different welding powers.

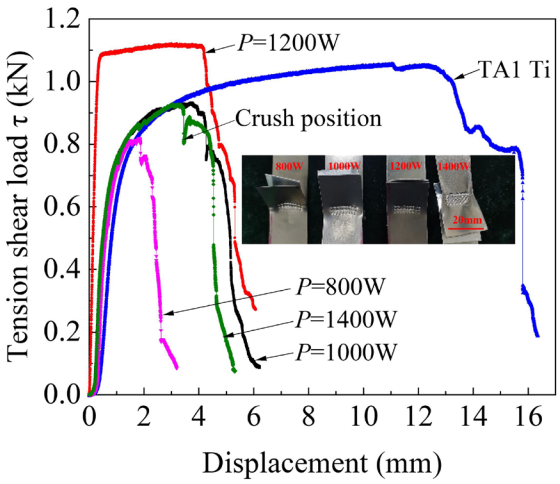

Figure 8. Force–displacement curve.

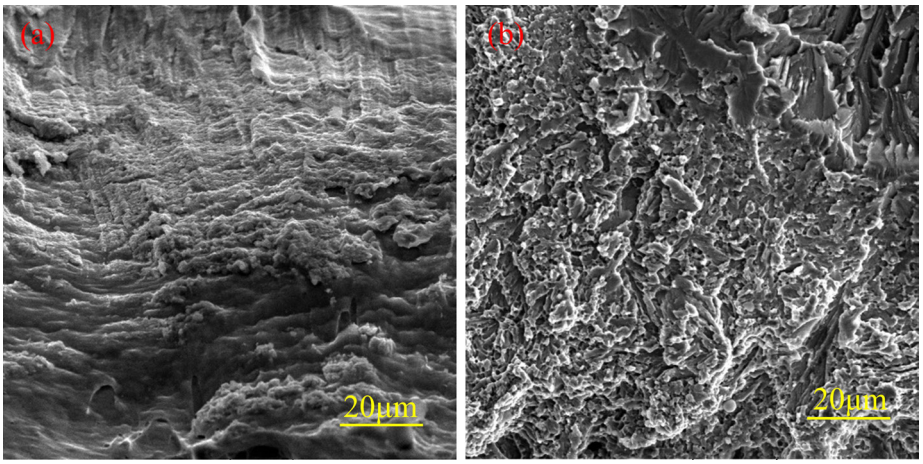

Figure 9. The interfacial fracture morphology of the Ti/Al/Ti welded joint (a) 1200 W (b) 1400 W.

tearing ridges and ductile dimple-like patterns, which is a typical quasi-cleavage fracture mode.

Figure 10 presents the longitudinal microhardness distribution of the Ti/Al/Ti weld seam at welding powers of 1200 W and 1400 W. Due to the occurrence of recrystallization during the welding process, the microhardness of 1060Al decreases from 30 $HV_{0.025\,kg}$ to 21.2 $HV_{0.025\,kg}$, and there is no significant difference in the hardness distribution throughout the intermediate layer. This result is related to the previously mentioned thermal insulation effect of TA1 Ti, which ensures a uniform temperature distribution in the intermediate layer. At a power of 1200 W, the hardness values of the upper and lower titanium layers do not change significantly relative to that of the base material, and there is a slight increase in hardness near the sonotrode zone due to work hardening. However, at a power of 1400 W, the hardness of the upper TA1 layer decreases from 220 $HV_{0.025\,kg}$ to 203.4 $HV_{0.025\,kg}$ due to recrystallization, while the hardness of the lower TA1 layer remains unchanged. At the interface, when the welding power reaches 1400 W, the precipitation of $TiAl_2$+(Al) significantly increases the hardness. The theoretical hardness value of $TiAl_2$ is 16.285 GPa (1661.721 HV), while the hardness test value in this region is 355±19 $HV_{0.025\,kg}$, indicating that this region is a mixed phase of $TiAl_2$+ (Al). Increasing the welding power from 1200 W to 1400 W results in the formation of IMCs. This correlates with increased hardness but decreased tensile–shear strength and elongation, indicating a trade-off between hardness and ductility with varying welding power. As the precipitation of IMCs, the maximum hardness of the weld increases from 227±6 $HV_{0.025\,kg}$ to 355±19 $HV_{0.025\,kg}$, indicating a positive correlation. However, the tensile–shear strength decreases from 124.4 MPa to 103.3 MPa, and elongation drops from 5.9% to 4.7%, suggesting that IMCs leads to reduced ductility and strength. Figure 11 shows the SPM morphology and p-h curve for a typical phase of the nanoindentation near the sonotrode side at a welding power of 1400W. The residual indentation from the Ti side to the Al side shows a jump distribution (Figure 11a). The hardness on the Ti side is 0.69GPa, and the hardness in the intermediate layer is in a steady distribution and shows a lower value (2.64GPa). The material around the indentation of TA1 Ti and 1060 Al shows evidence of piling up, indicating good plasticity. The highest hardness is observed at the Ti/Al interface, reaching up to 3.48 GPa, and the deformation morphology around the indentation is similar to a shear band. As shown in Figure 11b, the $TiAl_2$+(Al) phase exhibits high hardness, and the indentation depth is 489.1 nm under the maximum load of 8000 μN. The variation in hardness at the interface is the result of increased dislocation density, IMC phase precipitation, and the accumulation of residual stress.

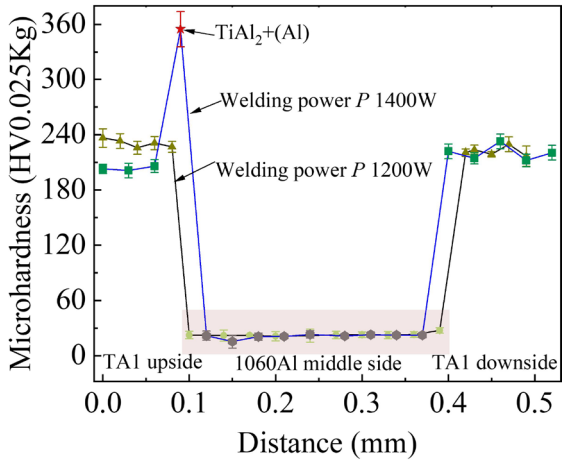

Figure 10. Microhardness of the Ti/Al/Ti weld in the longitudinal direction.

4. Conclusions

In this article, Ti/Al/Ti laminated composite materials using ultrasonic welding technology were successfully prepared. The influences of welding process parameters on the microstructures and properties of the weld joint were analyzed. Moreover, the mechanism of interface formation and the enhancement of joint performance due to constraint effects were investigated. The main conclusions are as follows:

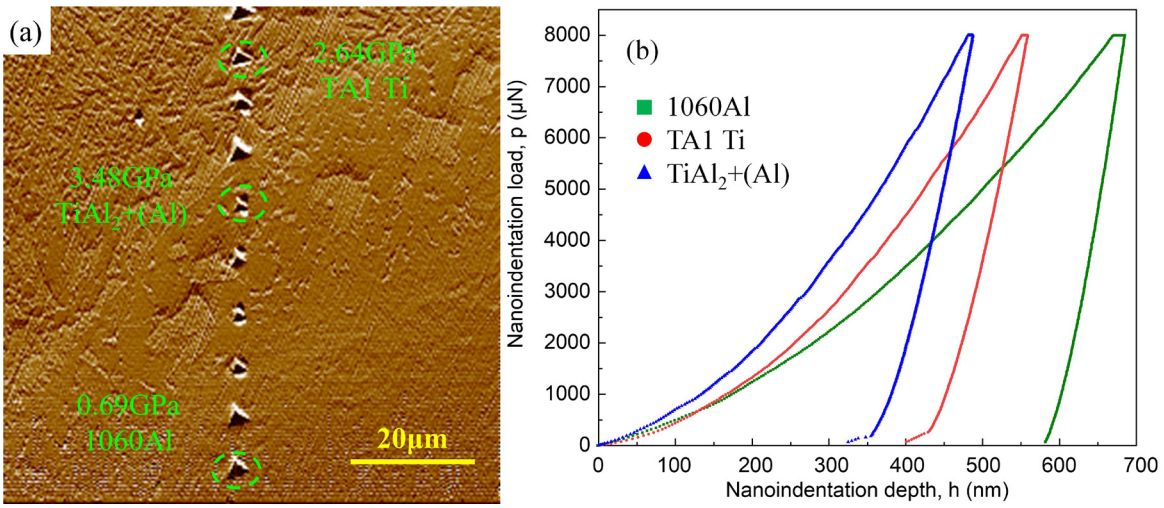

Figure 11. Nanoindentation results (a) SPM topography (b) P-h curves.

1. With the increase in welding power, the interface temperature increases from approximately 214 °C to 647 °C, which remains below the melting point of the base material. Additionally, the temperature difference between the upper and lower interfaces gradually decreases. In terms of microstructure and microhardness, the intermediate layer exhibits an approximately uniform distribution.
2. At a welding power of 1200 W, the presence of a titanium peninsula region in the aluminum layer indicates localized melting below the equilibrium melting point of aluminum. There are some vortex-like features at the joining interface. When the welding power reaches 1400 W, IMC phases ($TiAl_2$) precipitate at the interface.
3. The plastic constraint strengthening effect is most pronounced at a welding power of 1200 W. The joint achieves the highest tensile shear strength (124.4 MPa), which is 35.3% of the strength of the titanium base material and 113.1% of the strength of the aluminum base material.

5. Acknowledgments

This research was funded by the financial support from the National Natural Science Foundation of China (grant no. U1731118), the Science and Technology Research Project of Jiangxi Provincial Department of Education (GJJ190918) and Postgraduate Innovation Project of Nanchang University (CX2019005).

6. References

1. Li Y, Tang XH, Xu LD, Cui HC, Zhang RL. Interfacial behaviors and joint properties of the dual beam laser fusion brazing Ti6Al4V/AA7075 dissimilar metals. J Manuf Process. 2022;73:279-89.
2. Zhang ZJ, Huang J, Yao CW, Zhang X. Effect of Ag alloying on the microstructure and mechanical properties of laser welded-brazed Ti/Al dissimilar joints. Mater Sci Eng A. 2022;848:143359.
3. Xue X, Wu XY, Liao J. Hot-cracking susceptibility and shear fracture behavior of dissimilar Ti6Al4V/AA6060 alloys in pulsed Nd: YAG laser welding. Chin J Aeronauti. 2021;34(4):375-86.
4. Zhai WG, Ye CQ, Deng GP, Fang X, Li SK. Microstructure and mechanical properties investigations of pure titanium-aluminum alloy composite fabricated by explosive welding. J Mater Eng Perform. 2023. In press.
5. Nan XC, Zhao HY, Ma CY, Sun SL, Sun GD, Xu ZY, et al. Interface characterization and formation mechanism of Al/Ti dissimilar joints of refill friction stir spot welding. Int J Adv Manuf Technol. 2023;126(3-4):1539-51.
6. Meng XC, Xie YM, Sun SM, Ma XT, Wan L, Cao J, et al. Lightweight design: friction-based welding between metal and polymer. Acta Metall Sin. 2023;36(6):881-98.
7. Kimura M, Nakamura S, Kusaka M, Seo K, Fuji A. Mechanical properties of friction welded joint between Ti–6Al–4V alloy and Al–Mg alloy (AA5052). Sci Technol Weld Join. 2005;10(6):666-72.
8. Su ZZ, Zhu ZQ, Zhang YF, Zhang H. Analysis of microstructure and mechanical properties of AZ31B magnesium Alloy/AA6061 aluminum alloy welded joint by ultrasonic welding. Mater Res. 2021;24(2):e20200488.
9. Zhou L, Min J, He WX, Huang YX, Song XG. Effect of welding time on microstructure and mechanical properties of Al-Ti ultrasonic spot welds. J Manuf Process. 2018;33:64-73.
10. Zhang CQ, Robson JD, Ciuca O, Prangnell PB. Microstructural characterization and mechanical properties of high power ultrasonic spot welded aluminum alloy AA6111–TiAl6V4 dissimilar joints. Mater Charact. 2014;97:83-91.
11. Zhang CQ, Robson JD, Prangnell PB. Dissimilar ultrasonic spot welding of aerospace aluminum alloy AA2139 to titanium alloy TiAl6V4. J Mater Process Technol. 2016;231:382-8.
12. Balle F, Magin J. Ultrasonic Spot and torsion welding of aluminum to titanium alloys: process, properties and interfacial microstructure. Phys Procedia. 2015;70:846-9.
13. Wang SQ, Patel VK, Bhole SD, Wen GD, Chen DL. Microstructure and mechanical properties of ultrasonic spot welded Al/Ti alloy joints. Mater Des. 2015;78:33-41.
14. Mukhametgalina AA, Murzinova MA, Nazarov AA. Ultrasonic spot welded CP Ti/AA2024/CP Ti alloy joints. Lett Mater. 2021;11(4):508-13.
15. He XH, Shi HJ, Norfolk M. Influence of process parameters on bond properties of Al laminated structure produced by ultrasonic consolidation. Rapid Prototyping J. 2016;22(2):435-42.
16. Doherty RD, Hughes DA, Humphreys FJ, Jonas JJ, Jensen DJ, Kassner ME, et al. Current issues in recrystallization: a review. Mater Sci Eng A. 1997;238(2):219-74.
17. Anas NM, Dhindaw BK, Zuhailawati H, Abdullah TK, Anasyida AS. Effect of initial microstructure on properties of cryorolled Al 5052 alloy subjected to different annealing treatment temperatures. J Mater Eng Perform. 2018;27(11):6206-17.
18. Ohnuma I, Fujita Y, Mitsui H, Ishikawa K, Kainuma R, Ishida K. Phase equilibria in the Ti–Al binary system. Acta Mater. 2000;48(12):3113-23.
19. Kostov A, Živković D. Thermodynamic analysis of alloys Ti–Al, Ti–V, Al–V and Ti–Al–V. J Alloys Compd. 2008;460(1-2):164-71.
20. Wang TH, Sinha S, Komarasamy M, Shukla S, Williams S, Mishra RS. Ultrasonic spot welding of dissimilar Al 6022 and Al 7075 alloys. J Mater Process Technol. 2020;278:116460.